Organic & Biomolecular Chemistry

PAPER

View Article Online
View Journal | View Issue

Cite this: *Org. Biomol. Chem.*, 2015, **13**, 2087

Conformational modulation of peptides using β-amino benzenesulfonic acid (^{S}Ant)†

Gowri Priya,[a] Amol S. Kotmale,[b] Debamitra Chakravarty,[c] Vedavati G. Puranik,[c] Pattuparambil R. Rajamohanan[b] and Gangadhar J. Sanjayan*[a]

Received 18th November 2014,
Accepted 2nd December 2014

DOI: 10.1039/c4ob02421d

www.rsc.org/obc

This communication describes the utility of a conformationally restricted aromatic β-amino acid (2-aminobenzenesulfonic acid, ^{S}Ant) inducing various folding interactions in short peptides. Sandwiching ^{S}Ant between diverse amino acid residues was shown to form robust folded architectures featuring a variety of H-bonded networks, suggesting its utility in inducing peptide folding.

Introduction

Nature rivets peptides to be the basic structural entities for numerous biological phenomena. Peptides feature complex folded structures as prerequisite criterion to exhibit their function.[1,2] Understanding the folding phenomenon is a complex task. Conformational investigation using unnatural amino acid building blocks would aid in unveiling the mysterious mechanisms employed by nature in accomplishing the biological functions.

Recent times have witnessed an increased attention for development of unnatural amino acid building blocks, which can induce folding in peptide molecules.[3] Unnatural amino acids play a crucial role in inducing turn formation in synthetic peptides. An excellent example of an unnatural α-amino acid that has been used to induce turns resulting in 3_{10} helical architectures in synthetic peptides is 2-aminoisobutyric acid (Aib).[4] The torsional constraints of Aib impart conformational rigidity to peptide sequences. Similarly, gabapentin (Gpn) is another unnatural amino acid with four degrees of torsional freedom that has become popular in inducing robust turns in peptides.[5] Conformationally restricted aromatic amino acids have also been shown to be useful in the *de novo* design of foldamers.[6,7] Herein, we report on our observations that substantiate the turn inducing ability of orthanilic acid (^{S}Ant) in synthetic peptides. When sandwiched between various amino acid residues, ^{S}Ant has been shown to induce folding affording various H-bonded networks. The conformational features of the synthetic peptide backbones containing orthanilic acid has been studied in solid, as well as, solution states (Fig. 1).

Results and discussion

Synthesis

Compounds **1–5**, required for the present study, were synthesized using multi-step synthetic strategies and **6** and **7** were synthesized by the segment doubling strategy, as depicted in Schemes 1–3 (ESI, page S3–S5†).

Conformational analysis

We synthesized peptides **1–5** wherein orthanilic acid is sandwiched by a combination of α and β amino acid residues (Fig. 1, *vide supra*). The idea of altering various amino acid residues around ^{S}Ant was to investigate its tolerance limit in promoting folding. The peptides **1** and **2** possess orthanilic acid on their backbone surrounded by two α-amino acids: Aib and Gly. The peptide **2** is a C-terminus amidated analogue of **1**. The peptide **3** was designed in such a way that orthanilic acid is sandwiched between cyclic α-amino acid Pro at the N-terminus and acyclic α-amino acid Gly at the C-terminus. Peptide **4** was designed and synthesized as a reversed sequence of **3** where the position of Pro and Ant was interchanged. Since anthranilic acid (Ant) is known to cause unexpected conformational changes when introduced at the N-terminus,[8] peptide **5** was also made in order to evaluate the conformational outcome.

[a]*Division of Organic Chemistry, National Chemical Laboratory, Dr Homi Bhabha Road, Pune 411 008, India. E-mail: gj.sanjayan@ncl.res.in; http://nclwebapps.ncl.res.in/gjsanjayan; Fax: +91-020-2590-2629; Tel: +91-020-2590-2082*
[b]*Centre for Materials Characterisation, National Chemical Laboratory, Dr Homi Bhabha Road, Pune 411 008, India*
[c]*Central NMR Facility, National Chemical Laboratory, Dr Homi Bhabha Road, Pune 411 008, India*

† Electronic supplementary information (ESI) available: ^{1}H, ^{13}C, DEPT-135 NMR, 2D study spectra, ESI mass spectra and theoretical study of new compounds are included. CCDC 978806–978810. For ESI and crystallographic data in CIF or other electronic format see DOI: 10.1039/c4ob02421d

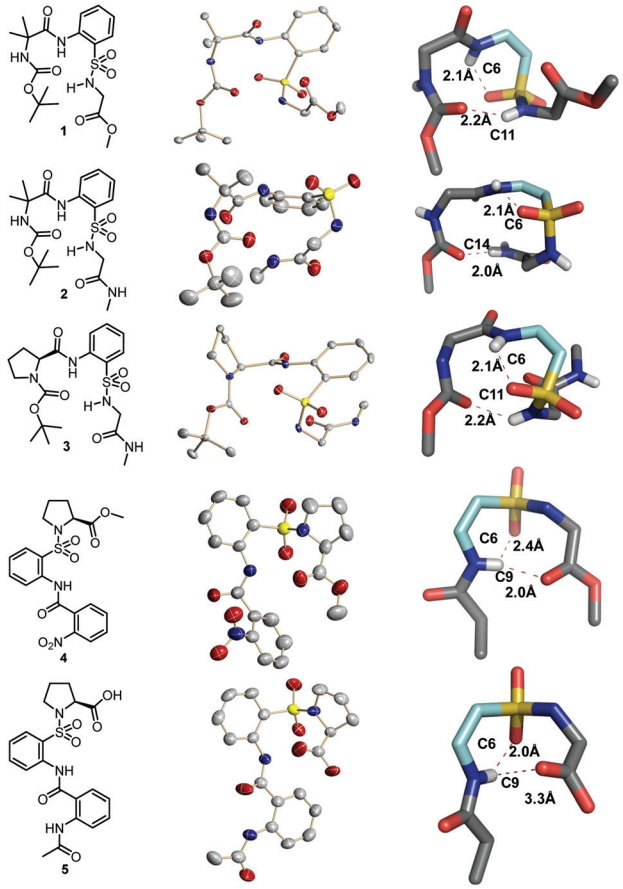

Fig. 1 Molecular structures of the peptides **1–5** (left), their ORTEP crystal structure diagrams (centre) and PyMOL-rendered zoomed perspectives of turn regions (only the backbone atoms shown) featuring a variety of H-bonding patterns (right). All hydrogens, except the polar ones, have been deleted for clarity. *Note*: The C═C backbone atoms of ^{s}Ant are highlighted in cyan in the PyMOL-rendered structures.

Solid-state X-ray studies of 1–5

Extensive efforts for crystallization led to the crystal formation in peptides **1–5**. It is evident from all the crystal structures that the peptides containing ^{S}Ant feature folded architectures with a variety of inter-residual hydrogen-bonded networks, in addition to the intra-residual 6-membered H-bonding present within the orthanilic acid residue, depending upon the amino acid to which ^{S}Ant is linked. The peptides exhibit folding mainly due to the conformational restriction imposed by ^{S}Ant having the closely positioned amino and sulfonamide groups – separated by a sp^2 bond, which is part of an aromatic ring. The peptides **1** and **3** adopt 11-membered H-bonded folding and the peptide **2**, although a C-terminus amidated analogue of peptide **1**, adopts a 14-membered H-bonded folding. It was observed that the crystal lattice of peptide **1** contained two molecules wherein one of the molecules exhibits a 11-membered inter-residual H-bond and another one with an almost similar folded architecture, but devoid of 11-membered inter-residual H-bond (ESI, S15†). The crystal structures of the peptides **4** and **5** clearly revealed a folded conformation featuring

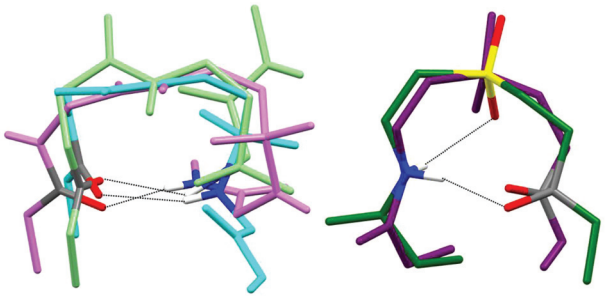

Fig. 2 Overlayed crystal structures of peptides **1–3** (left), featuring a C_{11} H-bonding and **4** and **5** (right), featuring a C_9 H-bonding. *Note*: The peptides **1–5** are highlighted as cyan, magenta, light green, purple and dark green, respectively. All hydrogens, except the polar ones, have been deleted for clarity, and the acceptor and donor atoms involved in hydrogen-bonding are highlighted.

an inter-residual 9-membered H-bonding. The fold adopted by the peptide **4** remains intact even after acetylating the N-terminus of the peptide as in **5**, without disturbing the H-bonding pattern on the folded backbone. It is clearly evident from the crystal structures of the peptides that the orthanilic acid containing peptides adopt rigid folded architectures featuring inter-residual H-bonds, which might be attributed to the torsional flexibility of the sulphonamide group varying from −88.9° (as in peptide **5**) to 99.9° (as in peptide **2**) present on the peptide backbones. The inter-residual H-bonding distance $[d(\mathrm{H}\cdots\mathrm{A})_{av}]$ observed in the peptides is 2.38 Å. The hydrogen-bonding angle $[\Delta(\mathrm{D}-\mathrm{H}\cdots\mathrm{A})]$ varies from 138° (as in peptide **3**) to 173° (as in peptide **2**). Although folding is prevalent in all the structures **1–5**, the structural disparity in their H-bonded network is evident from the overlayed crystal structures. Whereas peptides **1–3** form an extended β-turn-like structure featuring 11-membered H-bonding, peptides **4** and **5** form a *pseudo* β-turn structure featuring 9-membered H-bonding (Fig. 2).

Solution-state NMR studies of 1–5

Conformational investigation of the peptides in the solution-state was studied using 2D NMR experiments. The characteristic inter-residual nOes clearly revealed the folded conformations of the peptides, as seen in the solid-state. All the compounds were readily soluble in non-polar organic solvents (≫100 mM in $CDCl_3$) at room temperature suggesting the hydrogen bonding groups to be strongly shielded, preventing the formation of molecular aggregates. The presence of the inter-residual H-bonding was substantiated by the $[D_6]$-DMSO titration studies of **1**, **2**, **3**, and **5** ($\Delta\delta < 0.2$ ppm) (ESI S49–S54†) and variable temperature studies of the peptides **1**, **2**, **3** and **5** (268–323° K; $\Delta\delta/\Delta T < -2$ ppb K^{-1}) (ESI S55–S60†). The peptides **1**, **2**, **3** and **5** showed sharp signals rendering their conformational analysis easy. The diagnostic long range inter-residual nOes that supported the folded conformations of the peptides in solution state for **2** are: C13H *vs.* NH1, C14H *vs.* NH2, ^{t}Boc(H) *vs.* NH4, ^{t}Boc(H) *vs.* NH2 and ^{t}Boc(H) *vs.* C10H

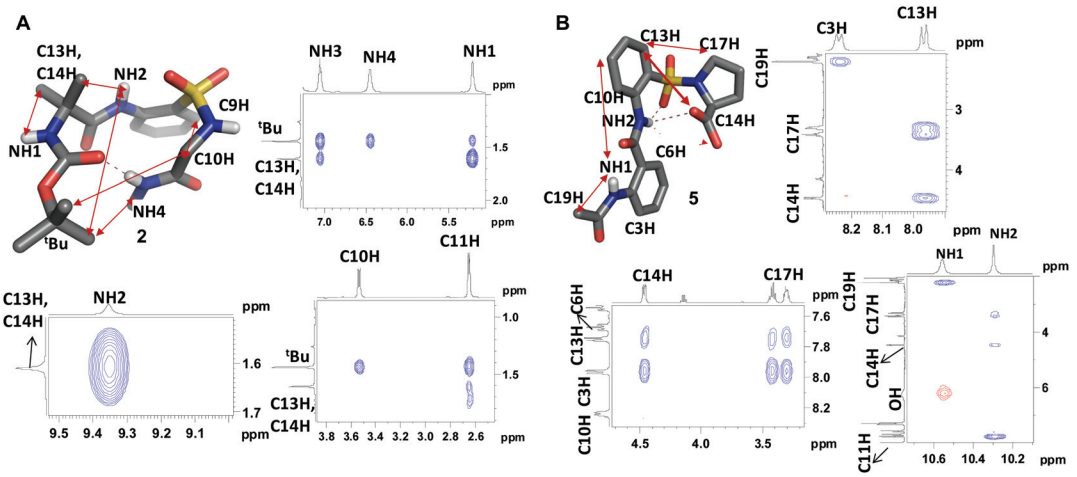

Fig. 3 (A) Crystal structure of **2** and its selected 2D NOESY excerpts supporting folded conformation. (B) Crystal structure of **5** and its selected 2D NOESY excerpts supporting folded conformation (500 MHz, $CDCl_3$).

(Fig. 3A) and for **5** are: C13H *vs.* C17H and C13H *vs.* C14H (Fig. 3B).

MD simulation studies of 7 and 8

We also synthesised higher order oligomers **6** and **7** (Fig. 4) corresponding to the folded peptides **2** and **3** to gain insight into their conformational features. All efforts to crystallize the oligomers **6** and **7** went in vain. Thus, the solution-state conformational investigation of these oligomers was done using NOE-based MD simulation studies employing the distance constraints (ESI S81–S85†). The signal assignments were done using a combination of 2D NOESY, COSY, TOCSY, HMBC and HSQC experiments. The inter-residual nOes observed in the 2D solution-state NMR experiments supported the 11-membered H-bonding on their backbones and revealed helically folded architectures for the oligomers **6** (Fig. 3A) and **7** (Fig. 4B).

The conformation observed in the crystal structures of **2** and **3** is perfectly reproduced by MD simulation studies as shown by the overlay of the crystal structures and their respective minimum energy structures obtained from the NOE-based simulation studies (ESI S81–S83†). The good agreement between the simulated structures and experimental structural data of **2** (RMSD < 0.2) and **3** (RMSD < 0.1), validates the reliability of MD simulation methods for accurate prediction of the solution-state conformation of peptides as illustrated in the case of several peptide oligomers in the literature.[9]

CD studies of 3 and 7

The circular dichroism spectra provided the characteristic signature supporting the helical conformations of the peptides **3** and **7** (Fig. 5).

The peptide **3** displayed a maxima at 194 nm, zero crossing at 195 nm and minima at 212 nm. The oligomer **7** displayed a

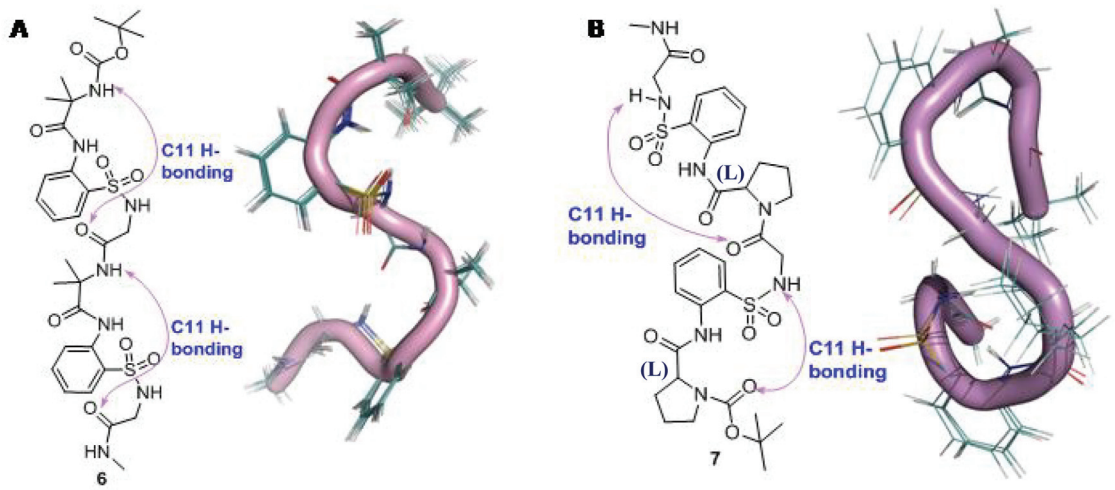

Fig. 4 (A) Molecular structure of hexapeptide **6** and its cartoon representation of 20 superimposed minimum energy structures. (B) Molecular structure of hexapeptide **7** and its cartoon representation of 20 superimposed minimum energy structures.

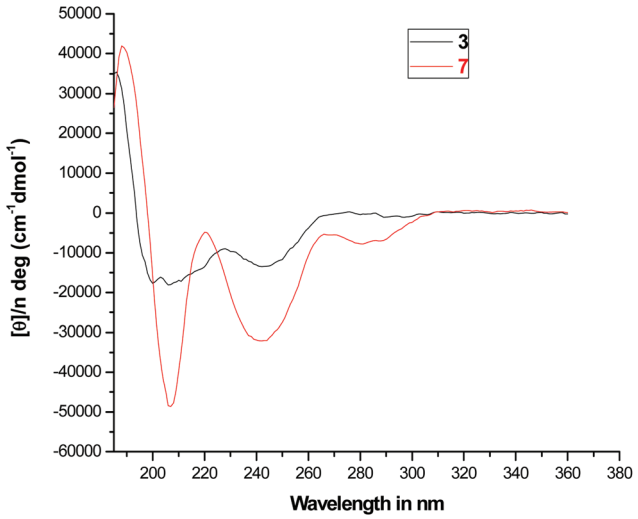

Fig. 5 CD spectra of the peptides **3** and **7** recorded in MeOH at 298 K using 0.2 mM concentrated solutions.

maxima at 198 nm, zero crossing at 200 nm and minima at 218 nm. A strong cotton effect was also observed (second minima) at 240 nm for the peptides **3** and **7**, presumably owing to the backbone aromatic electronic transitions in the peptide oligomers.

Conclusions

In conclusion, this work provides insight into the folding interactions caused by orthanilic acid in peptides. When sandwiched between amino acids, this conformationally rigid β-amino sulfonic acid has been shown to induce folding featuring a variety of hydrogen-bonded networks, as evident from crystal structure[10] and NMR studies. The results described herein suggest that orthanilic acid, a commercially easily available and inexpensive unnatural amino acid, offers good promise of inducing folding interactions in peptides.

Experimental procedures

Crystal X-ray crystallographic studies

Crystallographic data for the compounds **1**, **2**, **3**, **4** and **5** were collected on SMART APEX-II CCD using Mo-Kα radiation (λ = 0.7107 Å) to a maximum θ range of 25.00°. Crystal to detector distance 5.00 cm, 512 × 512 pixels per frame, Oscillation per frame −0.5°, maximum detector swing angle = −30.0°, beam center = (260.2, 252.5), in plane spot width = 1.24, SAINT integration with different exposure time per frame and SADABS correction applied. All the structures were solved by direct methods using SHELXTL. All the data were corrected for Lorentzian, polarisation and absorption effects. SHELX-97 (ShelxTL) was used for structure solution and full matrix least squares refinement on F^2. Hydrogen atoms were included in the refinement as per the riding model.

Crystal data for 1. Single crystals of **1** were grown by slow evaporation of its solution in ethyl acetate and DCM. Colorless cube like crystals of approximate size 0.31 × 0.12 × 0.07 mm^3, were used for data collection. Multi-run data acquisition. Total scans = 4, total frames = 1271, Oscillation per frame −0.3°, exposure per frame = 15.0 s per frame, θ range = 2.23 to 25.00°, completeness to θ of 25.00° is 99.9%. $C_{18}H_{27}N_3O_7S$, M_W = 429.49, crystals belong to triclinic, space group $P\bar{1}$, a = 10.0269(3), b = 11.0127(3), c = 19.1212(5) Å, V = 2072.5(1) Å^3, Z = 4, D_c = 1.376 g cc^{-1}, (Mo-K$_\alpha$) = 0.201 mm^{-1}, 30 705 reflections measured, 7277 unique [$I > 2\sigma(I)$], R_1 = 0.036, wR_2 = 0.0829, largest diff. peak and hole 0.576 and −0.519 e Å^{-3}.

Crystal data for 2. Single crystals of **2** were grown by slow evaporation of the solution in ethyl acetate. Colorless needle like crystals of approximate size 0.42 × 0.25 × 0.12 mm^3, were used for data collection. Multi-run data acquisition. Total scans = 4, total frames = 1271, Oscillation per frame −0.3°, exposure per frame = 15.0 s per frame, θ range = 2.23 to 25.00°, completeness to θ of 25.00° is 100%. $C_{18}H_{28}N_4O_6S$, M_W = 428.5, crystals belong to monoclinic, space group $P21/c$, a = 15.5747(6), b = 9.4947(3), c = 15.4473(6) Å, V = 2141.33(14) Å^3, Z = 4, D_c = 1.329 g cc^{-1}, (Mo-K$_\alpha$) = 0.192 mm^{-1}, 16 008 reflections measured, 3775 unique [$I > 2\sigma(I)$)], R_1 = 0.0532, wR_2 = 0.1145, largest diff. peak and hole 0.286 and −0.347 e Å^{-3}.

Crystal data for 3. Single crystals of **3** were grown by slow evaporation of its solution in DCM and pet. ether. Colorless needle like crystals of approximate size 0.32 × 0.09 × 0.07 mm^3, were used for data collection. Multi-run data acquisition. Total scans = 4, total frames = 1559, exposure per frame = 10.0 s per frame, θ range = 2.53 to 25.00°, completeness to θ of 25.00° is 99.9%. $C_{19}H_{28}N_4O_6S$, M_W = 440.51, crystals belong to orthorhombic, space group $P2_12_12_1$, a = 9.2146(8) Å, b = 14.611(1) Å, c = 16.096(1) Å, V = 2166.9(3) Å^3, Z = 4, D_c = 1.35 g cc^{-1}, (Mo-K$_\alpha$) = 0.192 mm^{-1}, 9609 reflections measured, 3803 unique, [$I > 2\sigma(I)$)] R_1 = 0.0376, wR_2 = 0.0809, largest diff. peak and hole 0.389 and −0.425 e Å^{-3}.

Crystal data for 4. Single crystals of **4** were grown by slow evaporation of the solution in chloroform. Colorless plate like crystals of approximate size 0.42 × 0.31 × 0.08 mm^3, were used for data collection. Multi-run data acquisition. Total scans = 4, total frames = 1559, exposure per frame = 10.0 s per frame, θ range = 1.90 to 25.00°, completeness to θ of 25.00° is 99.9%. $C_{19}H_{19}N_3O_7S$, M_W = 433.43, crystals belong to monoclinic, space group $P2_1$, a = 7.5913(1) Å, b = 12.3192 (2) Å, c = 11.3409 (2) Å, V = 1004.34(3) Å^3, Z = 4, D_c = 1.433 g cc^{-1}, (Mo-K$_\alpha$) = 0.209 mm^{-1}, 14 526 reflections measured, 3527 unique, [$I > 2\sigma(I)$)] R_1 = 0.0344, wR_2 = 0.0857, largest diff. peak and hole 0.137 and −0.189 e Å^{-3}.

Crystal data for 5. Single crystals of **5** were grown by slow evaporation of the solution in acetone. Colorless needle like crystals of approximate size 0.43 × 0.19 × 0.1 mm^3, were used for data collection. Multi-run data acquisition. Total scans = 4, total frames = 1559, exposure per frame = 10.0 s per frame, θ range = 2.20 to 25.00°, completeness to θ of 25.00° is 99.9%. $C_{20}H_{21}N_3O_6S$, M_W = 431.46, crystals belong to monoclinic, space group $P2_1$, a = 10.3772(5) Å, b = 10.9443(5) Å, c =

17.4395(7) Å, V = 1979.93(15) Å^3, Z = 4, D_c = 1.447 g cc^{-1}, (Mo-K$_\alpha$) = 0.208 mm^{-1}, 14 978 reflections measured, 6559 unique, [$I > 2\sigma(I)$)] R_1 = 0.0388, wR_2 = 0.1001, largest diff. peak and hole 0.244 and −0.274 e Å^{-3}.

Acknowledgements

GP and ASK thank CSIR for fellowship. This work was funded by NCL-IGIB, New Delhi.

Notes and references

1 (*a*) G. N. Ramachandran and V. Sasisekharan, *Adv. Protein Chem.*, 1968, **23**, 283; (*b*) C. B. Anfinsen, *Science*, 1973, **181**, 223.

2 (*a*) C. M. Wilmot and J. M. Thornton, *J. Mol. Biol.*, 1988, **203**, 221; (*b*) K. C. Chou, *Anal. Biochem.*, 2000, **286**, 1.

3 (*a*) M. D. P. Risseeuw, M. Overhand, G. W. J. Fleet and M. I. Simone, *Amino Acids*, 2013, **45**, 613; (*b*) G. V. M. Sharma, V. B. Jadhav, K. V. S. Ramakrishna, P. Jayaprakash, K. Narsimulu, V. Subash and A. C. Kunwar, *J. Am. Chem. Soc.*, 2006, **128**, 14657; (*c*) W. S. Horne and S. H. Gellman, *Acc. Chem. Res.*, 2008, **41**, 1399; (*d*) A. Roy, P. Prabhakaran, P. K. Baruah and G. J. Sanjayan, *Chem. Commun.*, 2011, **47**, 11593; (*e*) T. A. Martinek and F. Fulop, *Chem. Soc. Rev.*, 2011, **41**, 687; (*f*) C. Tomasini, G. Angelici and N. Castellucci, *Eur. J. Org. Chem.*, 2011, 3648.

4 (*a*) C. Toniolo, M. Crisma, F. Formaggio and C. Peggion, *Biopolymers*, 2001, **60**, 396; (*b*) P. G. Vasudev, S. Chatterjee, N. Shamala and P. Balaram, *Chem. Rev.*, 2011, **111**, 657.

5 (*a*) P. G. Vasudev, S. Chatterjee, N. Shamala and P. Balaram, *Chem. Rev.*, 2010, **111**, 657; (*b*) P. G. Vasudev, K. Ananda, S. Chatterjee, S. Aravinda, N. Shamala and P. Balaram, *J. Am. Chem. Soc.*, 2007, **129**, 4039; (*c*) P. G. Vasudev, N. Shamala, K. Ananda and P. Balaram, *Angew. Chem., Int. Ed.*, 2005, **44**, 4972.

6 (*a*) Q. Gan, Y. Ferrand, C. Bao, B. Kauffmann, A. Grelard, H. Jiang and I. Huc, *Science*, 2011, **331**, 1172; (*b*) P. Prabhakaran, G. Priya and G. J. Sanjayan, *Angew. Chem., Int. Ed.*, 2012, **51**, 4006.

7 (*a*) P. Prabhakaran, S. S. Kale, V. G. Puranik, P. R. Rajamohanan, O. Chetina, J. A. K. Howard, H. J. Hofmann and G. J. Sanjayan, *J. Am. Chem. Soc.*, 2008, **130**, 17743; (*b*) S. S. Kale, G. Priya, A. S. Kotmale, R. L. Gawade, V. G. Puranik, P. R. Rajamohanan and G. J. Sanjayan, *Chem. Commun.*, 2013, **49**, 2222; (*c*) V. V. E. Ramesh, S. S. Kale, A. S. Kotmale, R. L. Gawade, V. G. Puranik, P. R. Rajamohanan and G. J. Sanjayan, *Org. Lett.*, 2013, **15**, 1504; (*d*) K. N. Vijayadas, H. C. Davis, A. S. Kotmale, R. L. Gawade, V. G. Puranik, P. R. Rajamohanan and G. J. Sanjayan, *Chem. Commun.*, 2012, **48**, 9747; (*e*) R. V. Nair, S. B. Baravkar, T. S. Ingole and G. J. Sanjayan, *Chem. Commun.*, 2014, **50**, 13874; (*f*) R. V. Nair, K. N. Vijayadas, A. Roy and G. J. Sanjayan, *Eur. J. Org. Chem.*, 2014, DOI: 10.1002/ejoc.201402877, and cited references therein.

8 V. V. E. Ramesh, G. Priya, A. S. Kotmale, R. G. Gonnade, P. R. Rajamohanan and G. J. Sanjayan, *Chem. Commun.*, 2012, **48**, 11205.

9 R. V. Nair, S. Kheria, S. Rayavarapu, A. S. Kotmale, B. Jagadeesh and R. G. Gonnade, *J. Am. Chem. Soc.*, 2013, **135**, 11477.

10 Crystallographic data of **1–5** have been deposited with the Cambridge Crystallographic Data Centre as supplementary publication no. 978806–978810 (for compounds **1–5**, respectively).